

# **Overview of Airborne-Electromagnetic and -Magnetic Geophysical Data Collection Using the TEMPEST<sup>®</sup> Survey Near Edmonton, Alberta**

# **Overview of Airborne- Electromagnetic and -Magnetic Geophysical Data Collection Using the TEMPEST® Survey near Edmonton, Alberta**

S.R. Slattery<sup>1</sup> and L.D. Andriashek<sup>2</sup>

<sup>1</sup> Formerly of Alberta Geological Survey (see page ii for current address)

<sup>2</sup> Energy Resources Conservation Board  
Alberta Geological Survey

June 2012

©Her Majesty the Queen in Right of Alberta, 2012  
ISBN 978-0-7785-8664-7

The Energy Resources Conservation Board/Alberta Geological Survey (ERCB/AGS), its employees and contractors make no warranty, guarantee or representation, express or implied, or assume any legal liability regarding the correctness, accuracy, completeness or reliability of this publication. Any reference to proprietary software and/or any use of proprietary data formats do not constitute endorsement by ERCB/AGS of any manufacturer's product.

If you use information from this publication in other publications or presentations, please acknowledge the ERCB/AGS. We recommend the following reference format:

Slattery, S.R. and Andriashek, L.D. (2012): Overview of airborne-electromagnetic and -magnetic geophysical data collection using the TEMPEST<sup>®</sup> survey near Edmonton, Alberta; Energy Resources Conservation Board, ERCB/AGS Open File Report 2012-11, 38 p.

**Author address:**

Shawn Slattery  
Syncrude Canada Ltd.  
P.O. Bag 4009, M.D. A 250  
Fort McMurray, AB T9H 3L1  
Canada  
Tel: 780.715.9579  
E-mail: [slattery.shawn@syncrude.com](mailto:slattery.shawn@syncrude.com)

**Published June 2012 by:**

Energy Resources Conservation Board  
Alberta Geological Survey  
4th Floor, Twin Atria Building  
4999 – 98th Avenue  
Edmonton, AB T6B 2X3  
Canada

Tel: 780.422.1927  
Fax: 780.422.1918  
E-mail: [AGS-Info@ercb.ca](mailto:AGS-Info@ercb.ca)  
Website: [www.ags.gov.ab.ca](http://www.ags.gov.ab.ca)

## Contents

Acknowledgements.....	v
Abstract.....	vi
1 Introduction.....	1
2 Purpose and Scope.....	1
3 Location of Study Area and Geophysical Study Blocks.....	4
4 Methodology.....	5
4.1 Data Acquisition, Processing and Interpretations.....	5
4.2 TEMPEST <sup>®</sup> Time-Domain Geophysical Survey.....	5
5 References.....	6
Appendix 1 – Logistics and Processing Report Airborne Magnetic and TEMPEST <sup>®</sup> Survey, Northeast Block–Edmonton Calgary Corridor, Alberta.....	8

## Table

Table 1. Data sources and types available to validate airborne-electromagnetic (AEM) and -magnetic (AM) geophysical data in the Edmonton–Calgary Corridor, Alberta.....	4
---	---

## Figures

Figure 1. Digital elevation model (DEM) accented by hillshaded relief of surface topography of the Edmonton–Calgary Corridor (ECC), Alberta.....	2
Figure 2. a) Location of the 11 geophysical survey blocks in the Edmonton–Calgary Corridor (ECC), Alberta. The type of geophysical survey completed and when it was completed are provided on each survey block. b) Location of the survey block near Edmonton, Alberta.....	3
Figure 3. Simplified, regional-scale cross-section, oriented west to east, of sediments and bedrock surveyed using the low-frequency, TEMPEST <sup>®</sup> time-domain survey, central Alberta.....	4
Figure 4. a) The TEMPEST <sup>®</sup> survey technique in flight.....	5

## **Acknowledgements**

Comments from T.G. Lemay and N. Atkinson of the Alberta Geological Survey improved an earlier version of this report. We also thank J. Dawson for editing the report.

## Abstract

This report is one in a series of eight Alberta Geological Survey (AGS) Open File reports that provide an overview of airborne-electromagnetic and -magnetic geophysical surveys completed over the Edmonton–Calgary Corridor (ECC) by Fugro Airborne Surveys. These surveys were completed between November 2007 to February 2010 as part of a joint AGS and Alberta Environment and Sustainable Resource Development (ESRD) study to determine the usefulness of the RESOLVE<sup>®</sup>, GEOTEM<sup>®</sup> and TEMPEST<sup>®</sup> geophysical survey techniques in mapping the distribution and physical attributes of sediment- and bedrock-aquifer complexes over areas of formerly glaciated terrain.

The ECC was selected as the first test area to support the AGS-ESRD groundwater mapping program as it represents the region with the highest rates of industrial and urban growth in the province. Since this growth will exert increasing demands on water resources in the ECC, it is necessary to reassess the spatial distribution of previously mapped, as well as unmapped, aquifer complexes in the region. By doing so, Alberta may better predict and manage current and/or future stresses on existing aquifer systems caused by industrial, agricultural and urban development. Airborne geophysical survey methods were selected as one of the tools in completing this assessment.

The ECC is an ideal area to evaluate the usefulness of airborne-electromagnetic and -magnetic geophysical survey techniques due to the wealth of existing surficial and subsurface geological datasets (i.e., geological mapping, lithologs, petrophysical data, field observations, etc.). These datasets provide users with a means to calibrate and verify airborne geophysical data, analyses and interpretations within the ECC.

This report describes data collection methods using the Fugro Airborne Surveys' TEMPEST<sup>®</sup> survey techniques and data processing completed for a survey block completed near Edmonton, Alberta.

## 1 Introduction

In recognition of increasing rates of urbanization and industrialization in Alberta, and the foreseeable pressures that this will have on existing water supplies, the Alberta Geological Survey (AGS) in partnership with Alberta Environment and Sustainable Resource Development (ESRD) has initiated a multiyear project to characterize nonsaline aquifer complexes within the province. The Edmonton–Calgary Corridor (ECC), the region with the most industrial and urban development in Alberta, was selected as the first study area by the AGS and ESRD (Figure 1).

It is inevitable that future groundwater use in the ECC will place additional stress on existing aquifer systems. Therefore, reassessing previously mapped aquifers, potentially locating unmapped aquifers and implementing management strategies that ensure groundwater resources exist for future use are essential. As management strategies and decision-making tools will require more accurate geological and hydrogeological models, innovative approaches to data collection will be required. In complicated geological terrains, such as the ECC, where hydraulic pathways within glacial sediments and between glacial sediments and underlying bedrock formations are poorly understood, continuous high-resolution geological mapping of both glacial sediments and bedrock formations is necessary to better understand and illustrate the architecture of geological strata. A better understanding of the geological architecture within the ECC will allow for improved geological modelling, which in turn will allow for a better hydrogeological model of the ECC. It is anticipated that this model will form the cornerstone for numerous applications, such as groundwater exploration programs, aquifer protection studies and significant recharge area identification. More importantly, this model will form the framework for groundwater-flow modelling exercises and future water-budget calculations leading to improved water management decisions.

Recognizing the need for high-quality regional geological data, AGS and ESRD have collaborated to obtain airborne-geophysical survey data for near-continuous coverage of the ECC. A similar approach has been taken in other areas of formerly glaciated terrain by geological surveys in the United States, Europe and the United Kingdom (cf., Smith et al., 2003, 2006, 2007; Lahti et al., 2005; Wiederhold et al., 2009). Despite the success of these surveys in mapping the distribution of near-surface and subsurface aquifers, one of the main objectives of our investigation is to evaluate and compare the usefulness of these same types of airborne-geophysical survey techniques in mapping the distribution of aquifers in the ECC.

Between November 2007 and February 2010, airborne-electromagnetic (AEM) and airborne-magnetic (AM) surveys were completed by Fugro Airborne Surveys over 11 study blocks in the ECC on behalf of AGS and ESRD. The airborne-geophysical surveys were undertaken using one or a combination of the following survey techniques: fixed-wing, GEOTEM<sup>®</sup> or TEMPEST<sup>®</sup> time-domain or helicopter-borne, RESOLVE<sup>®</sup> frequency-domain (Figure 2a).

This report provides an overview of data collection using the TEMPEST<sup>®</sup> time-domain survey technique, data processing and the interpretation of data completed over a study block near Edmonton, Alberta (Figure 2b). Information on RESOLVE<sup>®</sup> frequency-domain and/or GEOTEM<sup>®</sup> and TEMPEST<sup>®</sup> time-domain airborne-geophysical survey techniques completed over the remaining survey blocks in the ECC are presented in separate Open File reports (Slattery and Andriashek, 2012a–g).

## 2 Purpose and Scope

The reasons for completing AEM and AM geophysical surveys in the ECC are multifaceted. First, it is to evaluate the effectiveness of frequency- and time-domain geophysical surveys to determine the spatial distribution of near-surface and subsurface electrical and magnetic properties of sediments and bedrock. It is anticipated that these properties will be related to geological and hydrogeological features in the ECC,

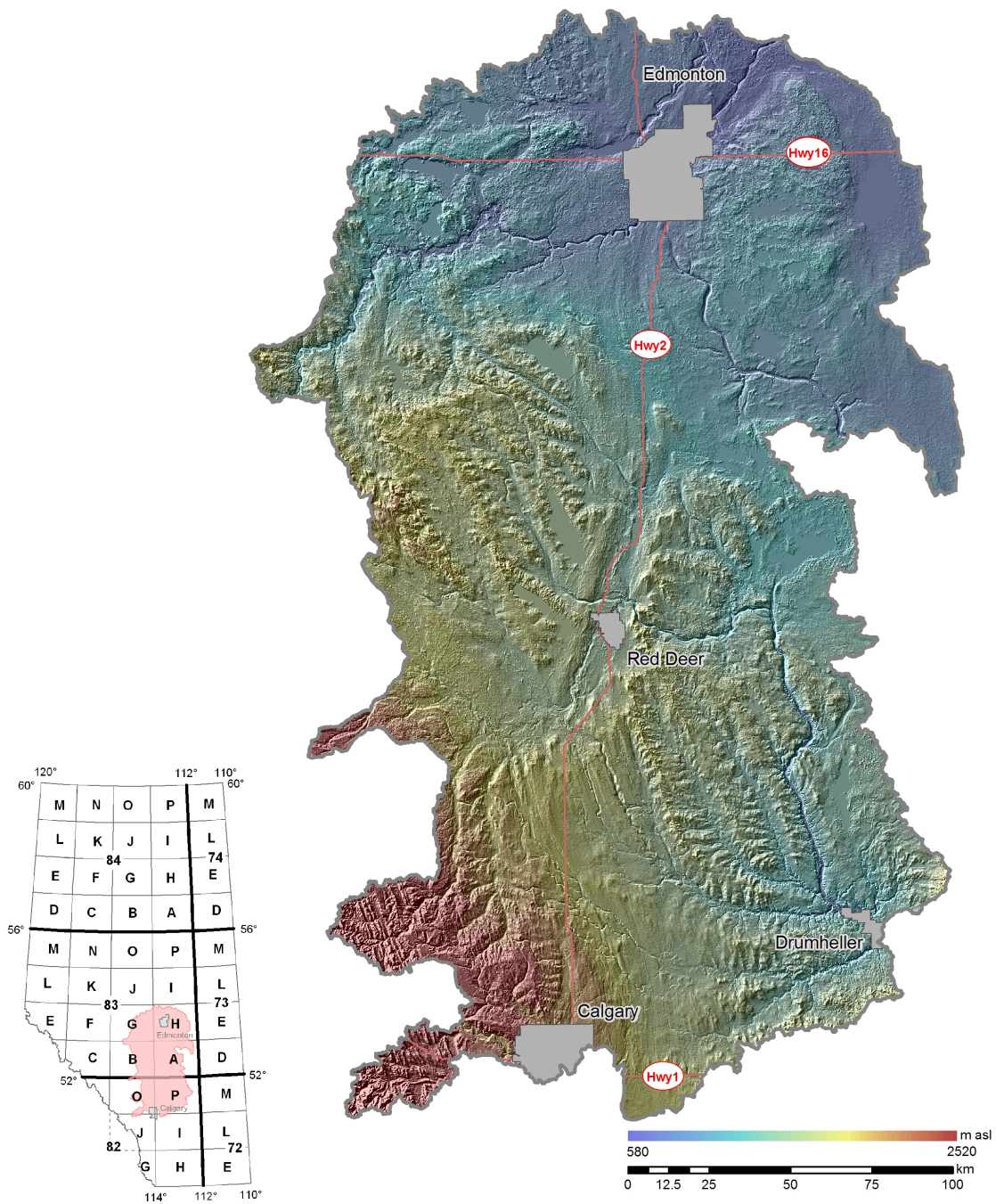
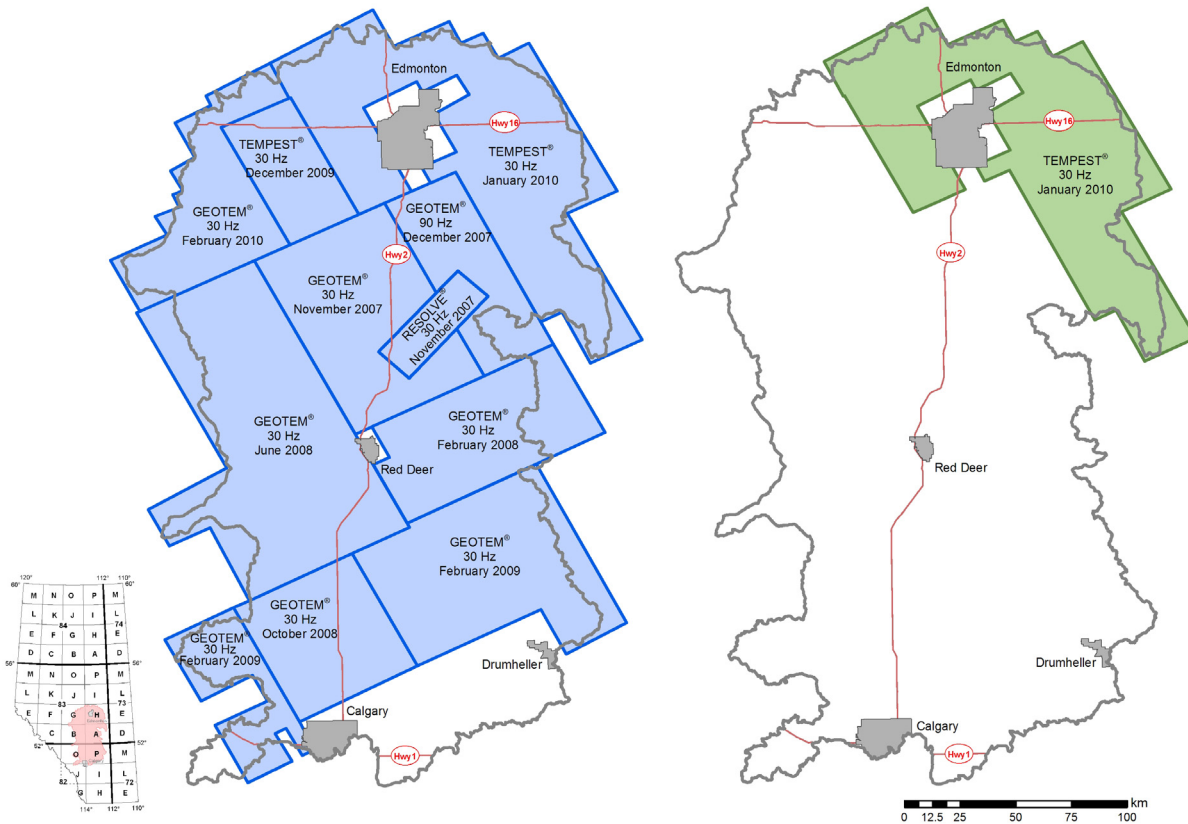


Figure 1. Digital elevation model (DEM) accented by hillshaded relief of surface topography of the Edmonton–Calgary Corridor (ECC), Alberta. Elevation of surface topography in metres above sea level is defined by colour ramp. Vertical exaggeration is 20x. Inset map depicts location of the ECC, Alberta.



**Figure 2. a) Location of the 11 geophysical survey blocks in the Edmonton–Calgary Corridor (ECC), Alberta. The type of geophysical survey completed and when it was completed are provided on each survey block. b) Location of the survey block near Edmonton, Alberta. Inset map depicts location of the ECC, Alberta.**

which will provide a better understanding of the geological architecture. This, in turn, will allow for more accurate geological and hydrogeological models to support improved water management decisions.

Second, the selection of the ECC for AEM and AM surveying was influenced by the widespread availability of existing surface and subsurface geological and geophysical data in the region (Table 1). These data are needed to validate the results and interpretations of the AEM and AM survey data. If the interpretation of AEM and AM survey data correlates with geological data and ground and downhole geophysical data, then AEM and AM surveying techniques could be used to interpret the geological framework in those areas that have limited subsurface geological and geophysical data. In such areas, AEM and AM surveys may provide a more time- and cost-efficient means to acquire continuous, high-quality geological data than traditional drilling methods and geological mapping investigations.

Third, the geological setting of the ECC is such that aquifer complexes can occur at various depths and have a variety of sediment and rock properties. Low-frequency (30 and 90 hertz [Hz]), TEMPEST® and GEOTEM® time-domain surveys were completed to provide greater penetration depths and summary electromagnetic (EM) and magnetic data to improve the delineation of regional-scale geological strata in the ECC. The AGS and ESRD tested the RESOLVE® frequency-domain survey in areas where more detailed resolution of the near-surface geology was required. A simplified cross-section of the geological setting is depicted in Figure 3.

**Table 1. Data sources and types available to validate airborne-electromagnetic (AEM) and -magnetic (AM) geophysical data in the Edmonton–Calgary Corridor, Alberta. Abbreviations: ESRD, Alberta Environment and Sustainable Resource Development; AGS, Alberta Geological Survey; ERCB, Energy Resources Conservation Board.**

Data Source	Data Class	Number of Data Points
ESRD digital water-well database	Water-well records and litholog records	234 902
AGS geotechnical database	Geotechnical borehole records	1202
ERCB oil-and-gas-well database	Oil-and-gas-well and petrophysical records	5161
AGS borehole database	Geological borehole and petrophysical records	363
AGS field observations	Field-based geological data	322

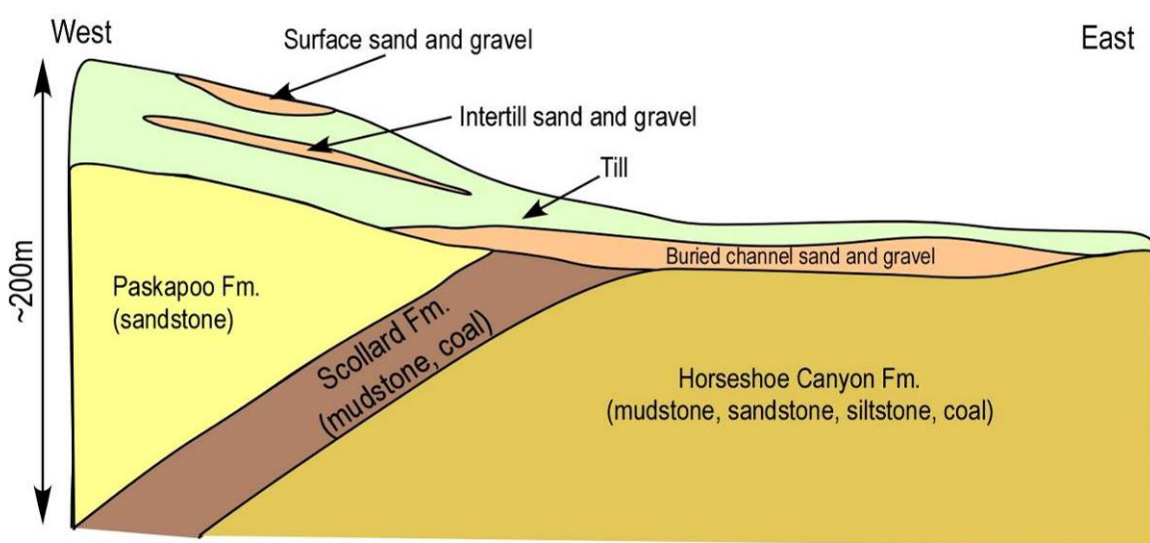


**Figure 3. Simplified, regional-scale cross-section, oriented west to east, of sediments and bedrock surveyed using the low-frequency, TEMPEST® time-domain survey, central Alberta.**

### 3 Location of Study Area and Geophysical Study Blocks

The ECC study area occupies approximately 49 500 km<sup>2</sup> and lies within portions of NTS 82I, J, O and P and 83A, B, G and H. Ten subwatershed boundaries define the irregularly shaped boundary of the ECC study area (Figure 1).

Between November 2007 and February 2010, AEM and AM surveys were completed over 11 study blocks in the ECC (Figure 2a). Data collection over the study block located near Edmonton (Figure 2b) was completed using a fixed-wing, TEMPEST® survey between January 18 and February 13, 2010. Data collection for the survey occurred over approximately 13 773 line-kilometres (line-km) using a base frequency of 30 Hz. Data were recorded along 176 flight lines ranging in length from 9 to 167 km, oriented northwest to southeast, with a line separation of approximately 800 m. Fourteen tie lines were completed with varying spacing in a northeast-southwest direction. Additional information on this survey technique is presented in the following section and in Appendix 1.

## 4 Methodology

### 4.1 Data Acquisition, Processing and Interpretations

Digital data from the AEM and AM surveys were acquired by the contractor, Fugro Airborne Surveys, using the TEMPEST<sup>®</sup> survey technique. This technique is briefly described below and presented in Appendix 1. For additional information, the reader is referred to Fraser (1978), Smith et al. (2003, 2006, 2007), Paine and Minty (2005) and Siemon (2006).

Datasets provided to AGS and ESRD from the contractor included both unprocessed and processed tabular datasets, as well as grid-based digital maps illustrating ground resistivity in relation to depth below ground surface. AGS and ESRD did not process any of the geophysical data.

### 4.2 TEMPEST<sup>®</sup> Time-Domain Geophysical Survey

The fixed-wing, TEMPEST<sup>®</sup> time-domain survey technique consists of a towed-bird EM system. The survey technique is based on the premise that fluctuations in the primary EM field produced in the transmitting loop will result in eddy currents being generated in any conductors in the ground. The eddy currents then decay to produce a secondary EM field that may be sensed in the receiver coil. Each primary pulse causes decaying eddy currents in the ground to produce a secondary magnetic field. This secondary magnetic field, in turn, induces a voltage in the receiver coils, which is the EM response. Good conductors decay slowly, whereas poor conductors decay more rapidly.

The primary EM pulses are created by a series of discontinuous sinusoidal current pulses fed into a three- or six-turn transmitting loop surrounding the aircraft and fixed to the nose, tail and wing tips. For this survey instrumentation was installed on a modified Casa 212 aircraft (Figure 4). The EM system is composed of a 30 channel multicoil system, as opposed to the 20 channel multicoil GEOTEM<sup>®</sup> system. The base frequency rate is selectable: 25, 30, 75, 90, 125, 150, 225 and 270 Hz, and the length of the pulse can be adjusted to suit specific targets. Standard pulse widths available are 0.6, 1.0, 2.0 and 4.0 ms, and the receiver is a three-axis (x, y, z) induction coil that is towed by the aircraft on a 135 m long, nonmagnetic cable. The usual mean terrain clearance for the aircraft is 120 m with the EM receiver normally being situated 50 m below and 130 m behind the aircraft. Additional information on the TEMPEST<sup>®</sup> survey technique is provided in Appendix 1.



Figure 4. a) The TEMPEST<sup>®</sup> survey technique in flight. Note the transmitting loop fixed to the aircraft's nose, tail and wing tips. Primary electromagnetic pulses are created by a series of discontinuous sinusoidal current pulses and transmitted into the transmitting loop. b) Modified Casa 212 aircraft used by Fugro Airborne Surveys in this study.

## 5 References

- Fraser, D.C. (1978): Resistivity mapping with an airborne multicoil electromagnetic system; *Geophysics*, v. 43, p. 144–172.
- Lahti, M., Vanhala, H., Mattsson, A., Beamish, D. and Lerssi, J. (2005): Environmental applications of airborne geophysics – groundwater and contaminated soil in Finland, Germany and United Kingdom; Geological Survey of Finland, Special Paper 39, p. 155–175.
- Paine, J.G. and Minty, B.R.S. (2005): Airborne hydrogeophysics; *in* *Hydrogeophysics*, Y. Rubin and S.S. Hubbard (ed.), Water Science and Technology Library, v. 50, p. 333–357.
- Siemon, B. (2006): Electromagnetic methods – frequency domain – airborne techniques; *in* *Groundwater geophysics – a tool for hydrogeology*, R. Kirsch (ed.), Springer-Verlag, p. 155–170.
- Slattery, S.R. and Andriashek, L.D. (2012a): Overview of airborne-electromagnetic and -magnetic geophysical data collection using the RESOLVE<sup>®</sup> and GEOTEM<sup>®</sup> survey techniques near Red Deer, central Alberta; Energy Resources Conservation Board, ERCB/AGS Open File Report 2012-07, 246 p.
- Slattery, S.R. and Andriashek, L.D. (2012b): Overview of airborne-electromagnetic and -magnetic geophysical data collection using the GEOTEM<sup>®</sup> survey technique in the Sylvan Lake area, central Alberta; Energy Resources Conservation Board, ERCB/AGS Open File Report 2012-08, 175 p.
- Slattery, S.R. and Andriashek, L.D. (2012c): Overview of airborne-electromagnetic and -magnetic geophysical data collection using the GEOTEM<sup>®</sup> survey technique north of Calgary, Alberta; Energy Resources Conservation Board, ERCB/AGS Open File Report 2012-09, 169 p.
- Slattery, S.R. and Andriashek, L.D. (2012d): Overview of airborne-electromagnetic and -magnetic geophysical survey data collection using the GEOTEM<sup>®</sup> survey technique near Three Hills and Cochrane, Alberta; Energy Resources Conservation Board, ERCB/AGS Open File Report 2012-10, 92 p.
- Slattery, S.R. and Andriashek, L.D. (2012e): Overview of airborne-electromagnetic and -magnetic geophysical data collection using the GEOTEM<sup>®</sup> survey technique near Drayton Valley, central Alberta; Energy Resources Conservation Board, ERCB/AGS Open File Report 2012-12, 92 p.
- Slattery, S.R. and Andriashek, L.D. (2012f): Overview of airborne-electromagnetic and magnetic-geophysical data collection and interpretation in the Edmonton–Calgary Corridor, Alberta; Energy Resources Conservation Board, ERCB/AGS Open File Report 2012-13, 208 p.
- Slattery, S.R. and Andriashek, L.D. (2012g): Overview of airborne-electromagnetic and -magnetic geophysical data collection using the TEMPEST<sup>®</sup> survey technique near Wabamun, central Alberta; Energy Resources Conservation Board, ERCB/AGS Open File Report 2012-14, 38 p.
- Smith, B.D., Irvine, R., Blome, C.D., Clark, A.K. and Smith, D.V. (2003): Preliminary results, helicopter electromagnetic and magnetic survey of the Seco Creek area, Medina and Uvalde counties, Texas; Proceedings for the Symposium on the Application of Geophysics to Environmental and Engineering Problems, San Antonio, Texas, 15 p.
- Smith, B.D., Thamke, J.N., Cain, M.J., Tyrrell, C. and Hill, P.L. (2006): Helicopter electromagnetic and magnetic survey maps and data, East Poplar Oil Field area, Fort Peck Indian Reservation, northeastern Montana, August 2004; United States Geological Survey, Open File Report 2006-1216, 23 p., 1 plate.
- Smith, B.D., Grauch, V.J.S., McCafferty, A.E., Smith, D.V., Rodriguez, B.R., Pool, D.R., Deszcz-Pan, M. and Labson, V.F. (2007): Airborne electromagnetic and magnetic surveys for ground-water

resources: a decade of study by the U.S. Geological Survey; *in* Proceedings of Exploration 07: Fifth Decennial International Conference on Mineral Exploration, B. Milkereit (ed.), p. 895–899.

Wiederhold, H., Schaumann, G. and Steuer, A. (2009): Airborne geophysical investigations for hydrogeological purposes in northern Germany; Near Surface 2009 – 15<sup>th</sup> European Meeting of Environmental and Engineering Geophysics, September 7–9, 2009, Dublin, Ireland, 5 p.

**Appendix 1 – Logistics and Processing Report Airborne Magnetic and TEMPEST®  
Survey, Northeast Block–Edmonton Calgary Corridor, Alberta**



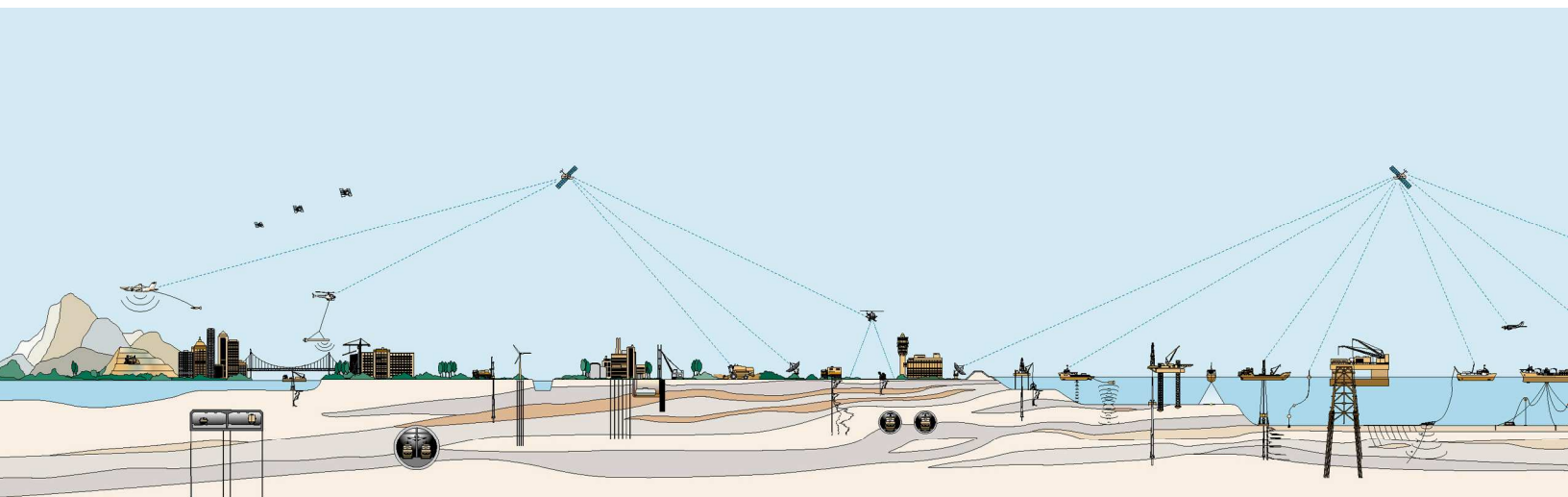
Fugro Airborne Surveys

**LOGISTICS AND PROCESSING REPORT**  
**Airborne Magnetic and TEMPEST® Survey**

**NORTHEAST BLOCK – EDMONTON CALGARY CORRIDOR**  
**ALBERTA**

**Job No. 10401**

Alberta Environment





**LOGISTICS AND PROCESSING REPORT  
AIRBORNE MAGNETIC AND TEMPEST® SURVEY  
NORTHEAST BLOCK – EDMONTON CALGARY  
CORRIDOR  
EDMONTON, ALBERTA**

**JOB NO. 10401**

Client: Alberta Environment, Water Policy Branch  
7<sup>th</sup> Floor, Oxbridge Place  
9820-106 Street  
Edmonton, Alberta  
T5K 2J6

Date of Report: March, 2010

# TABLE OF CONTENTS

<b>INTRODUCTION</b>	<b>5</b>
<b>SURVEY OPERATIONS</b>	<b>6</b>
Location of the Survey Area	6
Aircraft and Geophysical On-Board Equipment	7
Base Station Equipment	10
Field Office Equipment	10
Survey Specifications	10
Field Crew	11
Production Statistics	11
<b>QUALITY CONTROL AND COMPILATION PROCEDURES</b>	<b>12</b>
<i>Initial Field QC</i>	12
<i>Transmission of Data from Field to Office</i>	12
<b>DATA PROCESSING</b>	<b>13</b>
Flight Path Recovery	13
Altitude Data	13
Base Station Diurnal Magnetics	13
Airborne Magnetics	13
<i>Residual Magnetic Intensity</i>	14
<i>Magnetic First Vertical Derivative</i>	14
Electromagnetics	14
<i>dB/dt data</i>	14
<i>B-field data</i>	15
<i>Coil Oscillation Correction</i>	16
<i>Apparent Resistivity</i>	17
<i>Resistivity-Depth-Images (RDI)</i>	17
<b>FINAL PRODUCTS</b>	<b>18</b>
Digital Archives	18
Maps	18
Profile Plots	18
Report	18

# APPENDICES

- A DATA ARCHIVE DESCRIPTION
- B MAP PRODUCT GRIDS
- C REFERENCE WAVEFORM

# I

## Introduction

Between January 18<sup>th</sup> and February 13<sup>th</sup>, 2010, Fugro Airborne Surveys conducted a TEMPEST<sup>®</sup> electromagnetic and magnetic survey of the Northeast Block on behalf of the Alberta Environment. Using Edmonton, Alberta as the base of operations, a total of 13,773 line kilometres of data were collected using a Casa 212 modified aircraft (Figure 1).

The survey data were processed and compiled in the Fugro Airborne Surveys Ottawa office. The collected and processed data are presented on colour maps and multi-parameter profiles. The following maps were produced: Residual Magnetic Intensity (RMI), First Vertical Derivative of RMI, Resistivity Depth Slices at 0, 10, 30, 60 and 120 m, Apparent Resistivity and Flight Path. In addition, digital archives of the raw and processed survey data in line format, and gridded EM data were delivered.



Figure 1: Specially modified Casa 212 aircraft used by Fugro Airborne Surveys.

# II

## Survey Operations

### Location of the Survey Area

The Northeast Block of the Edmonton Calgary Corridor area (Figure 2) was flown with Edmonton, Alberta as the base of operations. A total of 176 traverse lines were flown, ranging in length from 9 km to 167 km, with a spacing of 800 m between lines, and 14 tie lines were flown with a varying spacing between tie lines totalling 13,773 km for the complete survey.

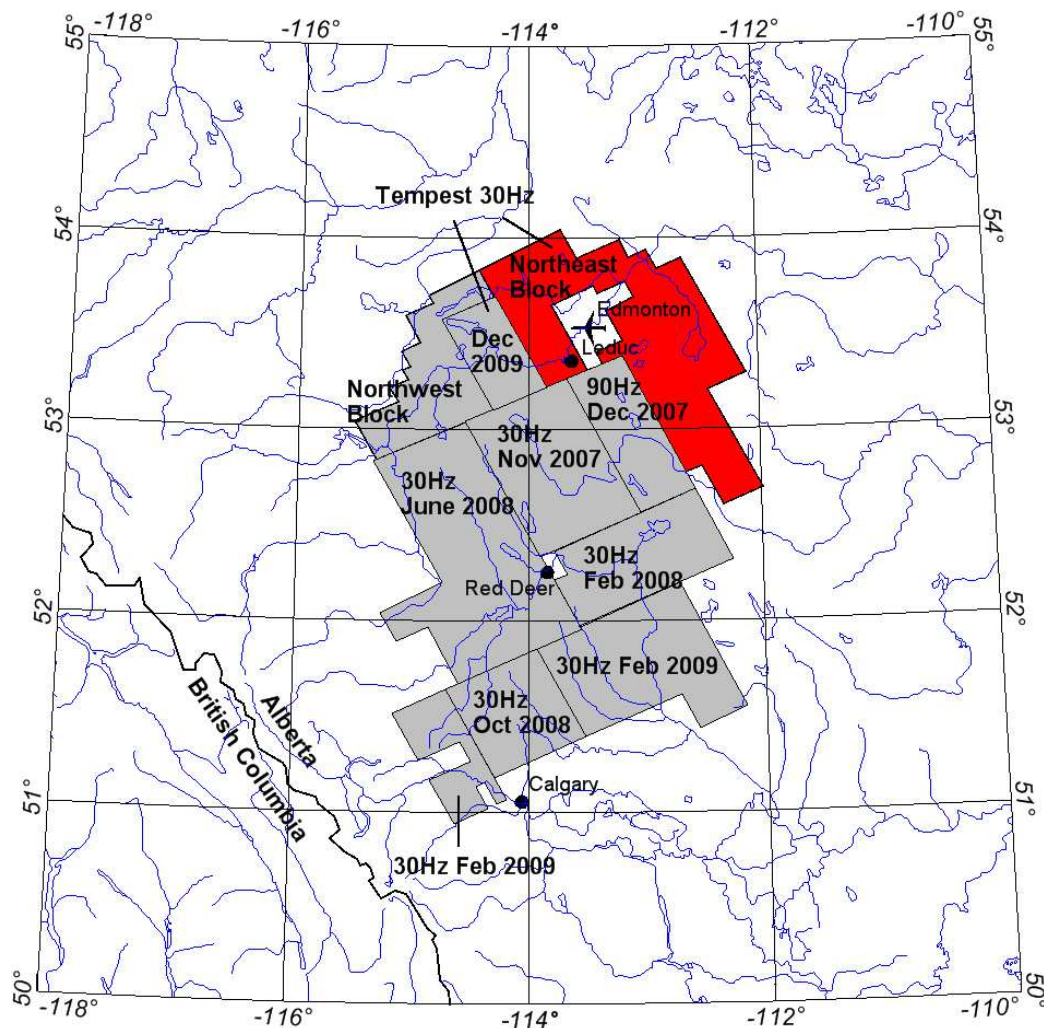


Figure 2: Survey location.

## Aircraft and Geophysical On-Board Equipment

Aircraft: Casa 212 (Twin Turbo Propeller)

Operator: FUGRO AIRBORNE SURVEYS

Registration: C-FDKM

Survey Speed: 125 knots / 145 mph / 65 m/s

Magnetometer: Scintrex Cs-2 single cell caesium vapour, towed-bird installation, sensitivity = 0.01 nT<sup>1</sup>, sampling rate = 0.1 s, ambient range 20,000 to 100,000 nT. The general noise envelope was kept below 0.5 nT. The nominal sensor height was ~73 m above ground.

Electromagnetic system: TEMPEST<sup>®</sup> 30 channel Multi-coil System

Transmitter: Vertical axis loop mounted on aircraft of 231 m<sup>2</sup>

Number of turns 1

Nominal height above ground of 120 m

Receiver: Multi-coil system (x, y and z) with a final recording rate of 4 samples per second, for the recording of 30 channels of x, y and z-coil data. The nominal height above ground is ~75 m, placed ~130 m behind the centre of the transmitter loop.

Base frequency: 30Hz

Waveform: Square

Half Cycle Duration: 16667 μs

Duty Cycle: 50%

Point value: 8.14μs

Transmitter Current: ~340 A

Dipole moment: 7.9x10<sup>4</sup> Am<sup>2</sup>



Figure 3: Mag and TEMPEST<sup>®</sup> Receivers



Figure 4: Modified Casa 212 in flight.

1 One nanotesla (nT) is the S.I. equivalent of one gamma.

Table 1: Electromagnetic Data Windows.

Channel	Start (p)	End (p)	Width (p)	Start (ms)	End (ms)	Width (ms)	Mid (ms)
1	1029	1041	13	8.366	8.472	0.106	8.419
2	1042	1043	2	8.472	8.488	0.016	8.48
3	1044	1045	2	8.488	8.504	0.016	8.496
4	1046	1049	4	8.504	8.537	0.033	8.521
5	1050	1054	5	8.537	8.577	0.041	8.557
6	1055	1060	6	8.577	8.626	0.049	8.602
7	1061	1067	7	8.626	8.683	0.057	8.655
8	1068	1075	8	8.683	8.748	0.065	8.716
9	1076	1085	10	8.748	8.83	0.081	8.789
10	1086	1097	12	8.83	8.927	0.098	8.879
11	1098	1111	14	8.927	9.041	0.114	8.984
12	1112	1127	16	9.041	9.172	0.13	9.106
13	1128	1145	18	9.172	9.318	0.146	9.245
14	1146	1165	20	9.318	9.481	0.163	9.399
15	1166	1187	22	9.481	9.66	0.179	9.57
16	1188	1211	24	9.66	9.855	0.195	9.757
17	1212	1237	26	9.855	10.07	0.212	9.961
18	1238	1265	28	10.07	10.3	0.228	10.18
19	1266	1295	30	10.3	10.54	0.244	10.42
20	1296	1330	35	10.54	10.82	0.285	10.68
21	1331	1370	40	10.82	11.15	0.326	10.99
22	1371	1415	45	11.15	11.52	0.366	11.33
23	1416	1465	50	11.52	11.92	0.407	11.72
24	1466	1520	55	11.92	12.37	0.448	12.15
25	1521	1580	60	12.37	12.86	0.488	12.61
26	1581	1650	70	12.86	13.43	0.57	13.14
27	1651	1730	80	13.43	14.08	0.651	13.75
28	1731	1820	90	14.08	14.81	0.732	14.45
29	1821	1920	100	14.81	15.63	0.814	15.22
30	1921	2048	128	15.63	16.67	1.042	16.15

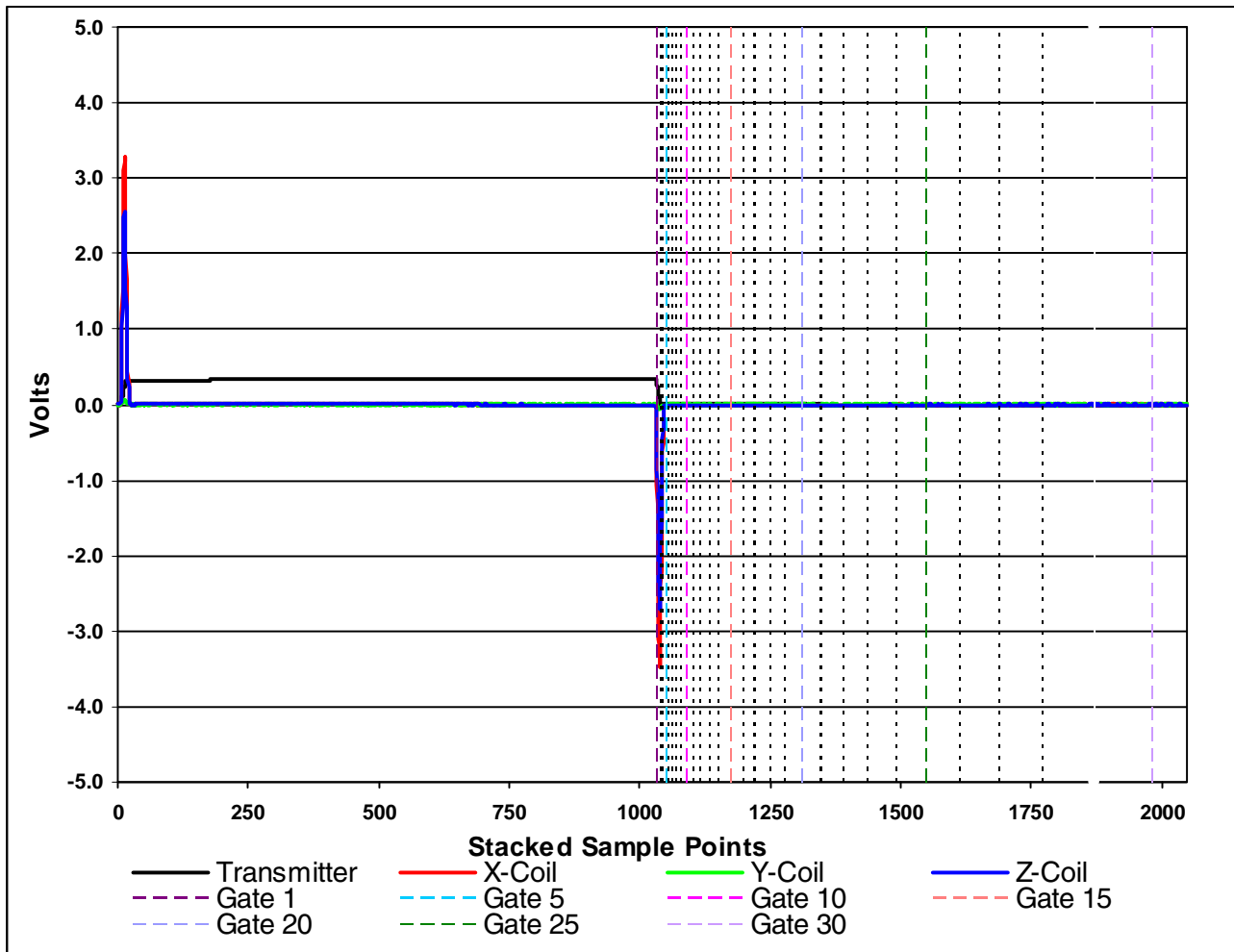


Figure 5: TEMPEST<sup>®</sup> Waveform and response with gate centres showing positions in sample points.

- Digital Acquisition: FUGRO AIRBORNE SURVEYS GEODAS SYSTEM.
- Barometric Altimeter: Rosemount 1241M, sensitivity 1 ft, 0.5 sec recording interval.
- Radar Altimeter: King, accuracy 2%, sensitivity 1 ft, range 0 to 2500 ft, 0.5 sec recording interval.
- Camera: Panasonic colour video, super VHS, model WV-CL302.
- Electronic Navigation: NovAtel OEM4, 1 sec recording interval, with a resolution of 0.00001 degree and an accuracy of  $\pm 5m$ .

### **Base Station Equipment**

Magnetometer:	Scintrex CS-2 single cell caesium vapour, mounted in a magnetically quiet area, measuring the total intensity of the earth's magnetic field in units of 0.01 nT at intervals of 0.5 s, within a noise envelope of 0.20 nT.
GPS Receiver:	NovAtel OEM4, measuring all GPS channels, for up to 12 satellites.
Computer:	Laptop, Pentium model or better.
Data Logger:	CF1, SBBS (single board base station).

### **Field Office Equipment**

Computer:	Dell Inspiron Series laptop.
Printer:	Bubblejet printer.
DVD writer Drive:	Internal DVD+RW format.
Hard Drives:	100 GB or bigger removable hard drive + two 500GB or bigger external hard drives for redundant backups.

### **Survey Specifications**

Traverse Line Direction:	150° - 330°
Traverse Line Spacing:	800 m
Tie Line direction:	065° - 245°
Tie Line spacing:	various
Navigation:	Real-Time Differential GPS. Traverse and tie line spacing was not to exceed the nominal by > 50 m for more than 3 km.
Altitude:	The survey was flown at a mean terrain clearance of 120 m. Altitude was not to exceed 140 m over 3 km.
Magnetic Noise Levels:	The noise envelope on the magnetic data was not to exceed $\pm$ 0.25 nT over 3 km.
EM Noise Levels:	The noise envelope on the raw electromagnetic B Field X- and Z-coil channel 30 was not to exceed $\pm$ 6000 fT over a distance greater than 3 km.

**Field Crew**

Pilots: B. Gorrel, M. Mellett  
Electronics Operator: E. Aparicio  
Engineer: T. Boughner

**Production Statistics**

Flying dates: January 18<sup>th</sup> – February 13<sup>th</sup>, 2009  
Total production: 13,773 line kilometres  
Number of production flights: 25  
Days lost weather: 9

# III

## Quality Control and Compilation Procedures

Important checks were performed during the data acquisition stage to ensure that the data quality was in keeping with the survey specifications. The following outlines the Quality Control measures conducted throughout the acquisition phase of the survey.

### Initial Field QC

At the completion of each day's flying an initial review of the data was performed in the field. This process was primarily to ensure all the equipment was functioning properly and enables the crew to immediately ascertain that production can resume the following day. This process does not necessarily determine if the data were within specifications. Priority was given to getting the data back to the office where a more thorough analysis of the data was performed. A list of the steps of the initial field review of the data follows:

- 1) All digital files were confirmed to be readable and free of defects.
- 2) The integrity of the airborne electromagnetic and magnetometer data was checked through statistical analysis and graphically viewed in profile form. Any null values or unreasonable noise levels were identified.
- 3) All altimeter and positional data were checked for any inconsistency, invalid values and spikes.
- 4) The base station files were examined for validity and continuity. The data extent was confirmed to cover the entire acquisition period.
- 5) The diurnal data were examined for any noise events or spiking.
- 6) Flight path video files were visually checked for quality and to confirm the full coverage for the survey flight.
- 7) Duplicate backups of all digital files were created.

### Transmission of Data from Field to Office

At the completion of each day's flying the raw data was uploaded to a secure FTP site. This enabled the office processing staff to immediately conduct more thorough data quality checks and start the processing with a minimum duplication of procedures or loss of time. This also enabled the direct supervision and involvement by senior processors and the availability of a greater depth of knowledge to be applied to any problems with the minimum of delay.

# IV

## Data Processing

### **Flight Path Recovery**

GPS Recovery:	GPS positions recalculated from the recorded raw range data, and differentially corrected in real-time.
Projection:	Alberta 10 TM Projection
Datum:	NAD83
Central meridian:	115° West
False Easting:	500000 metres
False Northing:	0 metres
Scale factor:	0.9992

### **Altitude Data**

Noise editing:	Alfatrim median filter used to eliminate the highest and lowest values from the statistical distribution of a 5 point sample window for the GPS elevation, and the two highest and lowest values from a 9 point sample window for the radar and barometric altimeters.
----------------	--

### **Base Station Diurnal Magnetics**

Noise editing:	Alfatrim median filter used to eliminate the two highest and two lowest values from the statistical distribution of a 9 point sample window.
Culture editing:	Polynomial interpolation via a graphic screen editor.
Noise filtering:	Running average filter set to remove wavelengths less than 2.5 seconds.
Extraction of long wavelength component:	Running average filter to retain only wavelengths greater than 71 seconds.

### **Airborne Magnetics**

Lag correction:	3.6 s
Noise editing:	4th difference editing routine set to remove spikes greater than 0.5 nT.
Noise filtering:	Triangular filter set to remove noise events having a wavelength less than 0.9 seconds.
Diurnal subtraction:	The long wavelength component of the diurnal (greater than 71 seconds) was removed from the data with a base value of 57875 nT added back.
IGRF removal date:	2010.1

Gridding: The data were gridded using an akima routine with a grid cell size of 200 m.

Near the Edmonton airport, the cultural interference was so severe that on some of the lines, the magnetic data were nulled out.

### **Residual Magnetic Intensity**

The residual magnetic intensity (RMI) is calculated from the total magnetic intensity (TMI), the diurnal, and the regional magnetic field. The TMI is measured in the aircraft, the diurnal is measured from the ground station and the regional magnetic field is calculated from the International Geomagnetic Reference Field (IGRF). The low frequency component of the diurnal is extracted from the filtered ground station data and removed from the TMI. The average of the diurnal is then added back in to obtain the resultant TMI. The regional magnetic field, calculated for the specific survey location and the time of the survey, is removed from the resultant TMI to obtain the RMI. The final step is to Tie line level and microlevel the RMI data.

### **Magnetic First Vertical Derivative**

The first vertical derivative was calculated in the frequency domain from the final grid values to enhance subtleties related to geological structures.

A first vertical derivative has also been displayed in profile form. This was calculated from the line data by combining the transfer functions of the 1st vertical derivative and a low-pass filter (cut-off wavelength = 5 seconds, roll-off wavelength = 7 seconds). The low-pass filter was designed to attenuate the high frequencies representing non-geological signal, which are normally enhanced by the derivative operator. This parameter is also stored in the final digital archive.

## **Electromagnetics**

### **dB/dt data**

Lag correction: 4.0 s

Data correction: The x, y and z-coil data were processed from the 30 raw channels recorded at 4 samples per second.

The following processing steps were applied to the dB/dt data from all coil sets:

- a) The data from channels 1 to 2 (on-time) and 3 to 30 (off-time) were corrected for drift in flight form (prior to cutting the recorded data back to the correct line limits) by passing a low order polynomial function through the baseline minima along each channel, via a graphic screen display;
- b) The data were edited for residual spheric spikes by examining the decay pattern of each individual EM transient. Bad decays (i.e. not fitting a normal exponential function) were deleted and replaced by interpolation;
- c) Noise filtering was done using an adaptive filter technique based on time domain triangular operators. Using a 2nd difference value to identify changes in gradient along each channel, minimal filtering (3 point convolution) is applied over the peaks of the anomalies, ranging in set increments up to a maximum amount of filtering in the resistive background areas (41 points for both the x-coil and the z-coil data);

- d) The filtered data from the x, y and z-coils were then re-sampled to a rate of 5 samples per second and combined into a common file for archiving.

## B-field data

### Processing steps:

The processing of the B-Field data stream is very similar to the processing for the regular dB/dt data. The lag adjustment used was the same, followed by:

- 1) Drift adjustments;
- 2) Spike editing for spheric events;
- 3) Correction for coherent noise. By nature, the B-Field data will contain a higher degree of coherency of the noise that automatically gets eliminated (or considerably attenuated) in the regular dB/dt, since this is the time derivative of the signal;
- 4) Final noise filtering with an adaptive filter.

*Note:* The introduction of the B-Field data stream, as part of the TEMPEST<sup>®</sup> system, provides the explorationist with a more effective tool for exploration in a broader range of geological environments and for a larger class of target priorities.

The advantage of the B-Field data compared with the normal voltage data (dB/dt) are as follows:

1. A broader range of target conductance that the system is sensitive to. (The B-Field is sensitive to bodies with conductance as great as 100,000 siemens);
2. Enhancement of the slowly decaying response of good conductors;
3. Suppression of rapidly decaying response of less conductive overburden;
4. Reduction in the effect of spherics on the data;
5. An enhanced ability to interpret anomalies due to conductors below thick conductive overburden;
6. Reduced dynamic range of the measured response (easier data processing and display).

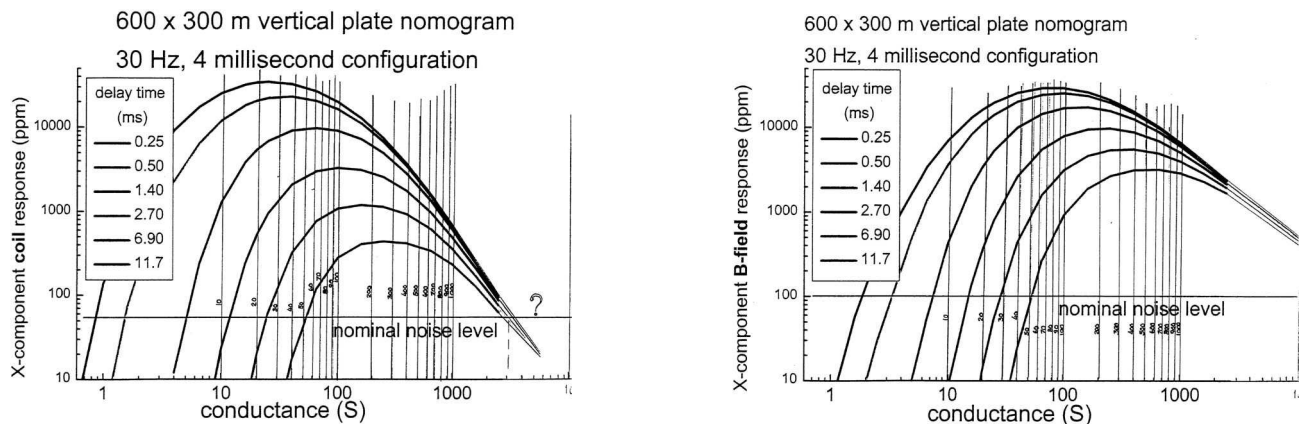


Figure 6: dB-dt vertical plate nomogram (left), B-field vertical plate nomogram (right).

Figure 6 displays the theoretical response of a vertical plate response for the dB/dt and B-Field signal. For the dB/dt response, you will note that the amplitude of the early channel peaks at about 25 siemens, and the late channels at about 250 siemens. As the conductance exceeds 1000 siemens the response curves quickly roll back into the noise level. For the B-Field response, the early channel amplitude peaks at about 80 siemens and the late channel at about 550 siemens. The projected extension of the graph in the direction of increasing conductance, where the response would roll back into the noise level, would be close to 100,000 siemens. Thus, a strong conductor, having a conductance of several thousand siemens, would be difficult to interpret on the dB/dt data, since the response would be mixed in with the background noise. However, this strong conductor would stand out clearly on the B-Field data, although it would have an unusual character, being a moderate to high amplitude response, exhibiting almost no decay.

Please note that because the TEMPEST<sup>®</sup> system uses a square-wave transmitter signal, the B-Field data is much better at representing the nature of the ground response. Although the dB/dt data is provided in the final database, this is considered as the raw measured data while generally most of the products are derived from the B-Field data.

### **Coil Oscillation Correction**

The electromagnetic receiver sensor is housed in a bird, which is towed behind the aircraft using a cable. Any changes in airspeed of the aircraft, variable crosswinds, or other turbulence will result in the bird swinging from side to side. This can result in the induction sensors inside the bird rotating about their mean orientation. The rotation is most marked when the air is particularly turbulent. The changes in orientation result in variable coupling of the induction coils to the primary and secondary fields. For example, if the sensor that is normally aligned to measure the x-axis response pitches upward, it will be measuring a response that will include a mixture of the X and Z-component responses. The effect of coil oscillation on the data increases as the signal from the ground (conductivity) increases and may not be noticeable when flying over areas which are generally resistive. This becomes more of a concern when flying over highly conductive ground.

Using the changes in the coupling of the primary field, it is possible to estimate the pitch, roll and yaw of the receiver sensors. In the estimation process, it is assumed that a smoothed version of the primary field represents the primary field that would be measured when the sensors are in the mean orientation. The orientations are estimated using a non-linear inversion procedure, so erroneous orientations are sometimes obtained. These are reviewed and edited to insure smoothly varying values of orientations. These orientations can then be used to unmix the measured data to generate a response that would be measured if the sensors were in the correct orientation. For more information on this procedure, see:

[http://www.fugroairborne.com/resources/technical\\_papers/airborne\\_em/atem.html](http://www.fugroairborne.com/resources/technical_papers/airborne_em/atem.html)

For the present dataset, the data from all 30 channels of dB/dt and B-Field parameters have been corrected for coil oscillation.

## Apparent Resistivity

Fugro has developed an algorithm that converts the response in any measurement window (on or off-time) into an apparent resistivity. This is performed using a look-up table that contains the response at a range of half-space conductivities and altimeter heights.

The apparent resistivity for the present dataset was calculated using dB/dt Z-Coil channels 1 - 30 to provide the maximum information on the near-surface resistivity of the ground which, when combined with the magnetic signature, provides good geological mapping.

## Resistivity-Depth-Images (RDI)

The Resistivity-Depth-Image (RDI) sections were calculated from the B-Field Z-coil response, using an algorithm that converts the response in any measurement window (on- or off-time) into resistivity. For on-time data, it is not straightforward to identify which depth the apparent resistivity is associated, or identify any variation in resistivity with depth. Hence, the earth is assigned a constant value from surface to depth.

However, for the off-time data, the apparent resistivity can be associated with a depth. This depth,  $\delta$ , depends on the magnetic permeability  $\mu$ , the delay time  $t$  of the measurement window and the estimated apparent conductivity  $\sigma_{app}$ , i.e.

$$\delta = 0.55 \sqrt{\frac{t}{\mu\sigma_{app}}}$$

The electromagnetic method is most sensitive to conductive features so resistive features will be poorly resolved. The process of converting voltage data to resistivity as a function of depth tends to create smoother depth variations than can occur in reality.

The RDI sections, derived from each survey line, are created as individual grids. An additional set of RDI grids have been corrected for altitude variations such that the top of each section reflects the true terrain topography and it is these grids that are displayed on the multi-parameter profiles.

The RDI derived information is also provided as SEG Y files and in a Geosoft database as an array. The array consists of 151 levels of resistivity, from 0 to 300 metres depth. The resistivity values can be gridded to provide resistivity depth slices for desired depths. On this project, resistivity-depth slices were created for depths of 0, 10, 30, 60 and 120 m below the surface.

# V

## Final Products

### Digital Archives

Line and grid data in the form of ASCII text files (\*.xyz), Geosoft databases (\*.gdb), SEG-Y Archives (\*.sgy), Geosoft grids (\*.grd), and ArcInfo ASCII grids (\*.asc) have been written to DVDs. The formats and layouts of these archives are further described in Appendix A (Data Archive Description). Hardcopies of all maps have been created as outlined below.

### Maps

Scale: 1:250,000  
Parameters: Residual Magnetic Intensity  
First Vertical Derivative of the Residual Magnetic Intensity  
Apparent Resistivity  
Resistivity Depth Slice at 0 m Depth  
Resistivity Depth Slice at 10 m Depth  
Resistivity Depth Slice at 30 m Depth  
Resistivity Depth Slice at 60 m Depth  
Resistivity Depth Slice at 120 m Depth  
Flight Path  
Media/Copies: 2 Paper & 2 Digital (Geosoft \*.map format & PDF Format)

### Profile Plots

Scale: 1:100,000  
Parameters: Multi-channel presentation with 28 channels of B-field X and Z-coil, Residual Magnetic Intensity, Calculated First Vertical Derivative, Radar Altimeter, EM Primary Field, Hz Monitor, Terrain and Terrain adjusted Resistivity Depth Section.  
Media/Copies: 1 Paper & 2 Digital (\*.png format) of Each Line

### Report

Media/Copies: 2 Paper & 2 digital (PDF format)

# Appendix A

---

## Data Archive Description

## Data Archive Description:

### Survey Details

Survey Area Name: Northeast Block – Edmonton Calgary Corridor  
Job number: 10401  
Client: Alberta Environment  
Survey Company Name: Fugro Airborne Surveys  
Flown Dates: January 18<sup>th</sup> – February 13<sup>th</sup>, 2009  
Archive Creation Date: March, 2010

### Survey Specifications

Traverse Line Azimuth: 150°-330°  
Traverse Line Spacing: 800 m  
Tie Line Azimuth: 065°-245°  
Tie Line Spacing: various  
Flying Elevation: 120 m Mean Terrain Clearance  
Average Aircraft Speed: 65 m/s

### Geodetic Information for map products

Projection: Alberta 10TM Projection  
Datum: NAD83  
Central meridian: 115° West  
False Easting: 500000 metres  
False Northing: 0 metres  
Scale factor: 0.9992  
I.G.R.F. Model: 2010  
I.G.R.F. Correction Date: 2010.1

### Equipment Specifications:

#### Navigation

GPS Receiver: NovAtel OEM4, 12 Channels  
Aircraft: Casa (Twin Turbo Propeller)  
Video Camera: Panasonic WV-CL302

#### Magnetics

Type: Scintrex CS-2 Caesium Vapour  
Installation: Towed bird  
Sensitivity: 0.01 nT  
Sampling: 0.1 s

## Electromagnetics

Type: TEMPEST®, 30 channel multi-coil system  
 Installation: Vertical axis loop (231m<sup>2</sup> area with 1 turn)  
 mounted on the aircraft.  
 Receiver coils in a towed bird.  
 Coil Orientation: X, Y and Z  
 Frequency: 30 Hz  
 Half Cycle Duration: 16667 µs  
 Duty Cycle: 50%  
 Geometry: Tx-Rx horizontal separation of ~130 m  
 Tx-Rx vertical separation of ~45 m  
 Sampling: 0.25 s

## Data Windows:

Channel	Start (p)	End (p)	Width (p)	Start (ms)	End (ms)	Width (ms)	Mid (ms)
1	1029	1041	13	8.366	8.472	0.106	8.419
2	1042	1043	2	8.472	8.488	0.016	8.48
3	1044	1045	2	8.488	8.504	0.016	8.496
4	1046	1049	4	8.504	8.537	0.033	8.521
5	1050	1054	5	8.537	8.577	0.041	8.557
6	1055	1060	6	8.577	8.626	0.049	8.602
7	1061	1067	7	8.626	8.683	0.057	8.655
8	1068	1075	8	8.683	8.748	0.065	8.716
9	1076	1085	10	8.748	8.83	0.081	8.789
10	1086	1097	12	8.83	8.927	0.098	8.879
11	1098	1111	14	8.927	9.041	0.114	8.984
12	1112	1127	16	9.041	9.172	0.13	9.106
13	1128	1145	18	9.172	9.318	0.146	9.245
14	1146	1165	20	9.318	9.481	0.163	9.399
15	1166	1187	22	9.481	9.66	0.179	9.57
16	1188	1211	24	9.66	9.855	0.195	9.757
17	1212	1237	26	9.855	10.07	0.212	9.961
18	1238	1265	28	10.07	10.3	0.228	10.18
19	1266	1295	30	10.3	10.54	0.244	10.42
20	1296	1330	35	10.54	10.82	0.285	10.68
21	1331	1370	40	10.82	11.15	0.326	10.99
22	1371	1415	45	11.15	11.52	0.366	11.33
23	1416	1465	50	11.52	11.92	0.407	11.72
24	1466	1520	55	11.92	12.37	0.448	12.15
25	1521	1580	60	12.37	12.86	0.488	12.61
26	1581	1650	70	12.86	13.43	0.57	13.14
27	1651	1730	80	13.43	14.08	0.651	13.75
28	1731	1820	90	14.08	14.81	0.732	14.45
29	1821	1920	100	14.81	15.63	0.814	15.22
30	1921	2048	128	15.63	16.67	1.042	16.15

**ASCII and Geosoft Line Archive File Layout (ERDA\_Northeast\_ascii.xyz & ERDA\_Northeast.gdb):**

Field	Variable	Description	Units
1	Line	Line Number	
2	Fiducial	Seconds after Midnight	sec.
3	Flight	Flight Number	-
4	Date	Date of the Survey Flight	ddmmyy
5	Lat_NAD83	Latitude in NAD83	degrees
6	Long_NAD83	Longitude in NAD83	degrees
7	X_NAD83	Easting (X) in NAD83 Alberta 10TM Projection	m
8	Y_NAD83	Northing (Y) in NAD83 Alberta 10TM Projection	m
9	GPS_Z	GPS Elevation (above WGS84 datum)	m
10	Radar	Radar Altimeter	m
11	DTM	Terrain (above WGS84 datum)	m
12	Diurnal	Ground Magnetic Intensity	nT
13	TMI_raw	Raw Airborne Total Magnetic Intensity	nT
14	IGRF	International Geomagnetic Reference Field	nT
15	RMI	Final Airborne Residual Magnetic Intensity	nT
16	Primary_field	Electromagnetic Primary Field	$\mu$ V
17	Hz_monitor	Powerline Monitor (60 Hz)	$\mu$ V
18-47	x01-x30	Final dB/dt X Coil Channels 1-30	pT/s
48-77	y01-y30	Final dB/dt Y Coil Channels 1-30	pT/s
78-107	z01-z30	Final dB/dt Z Coil Channels 1-30	pT/s
108-137	Bx01-Bx30	Final B Field X Coil Channels 1-30	fT
138-167	By01-By30	Final B Field Y Coil Channels 1-30	fT
168-197	Bz01-Bz30	Final B Field Z Coil Channels 1-30	fT
198-227	raw_x01-raw_x30	Raw dB/dt X Coil Channels 1-30	pT/s
228-257	raw_y01-raw_y30	Raw dB/dt Y Coil Channels 1-30	pT/s
258-287	raw_z01-raw_z30	Raw dB/dt Z Coil Channels 1-30	pT/s
288-317	raw_Bx01-raw_Bx30	Raw B Field X Coil Channels 1-30	fT
318-347	raw_By01-raw_By30	Raw B Field Y Coil Channels 1-30	fT
348-377	raw_Bz01-raw_Bz30	Raw B Field Z Coil Channels 1-30	fT
378	vd1	First Vertical Derivative of RMI	nT/m
379	res_hs_z	Apparent Resistivity (Half Space Model) Derived from dB/dt Z	ohm-m

Note – The null values in the ASCII archive are displayed as \*.

**ASCII and Geosoft RDI File Layout (ERDA\_Northeast\_RDI\_ascii.xyz and ERDA\_Northeast\_RDI.gdb):**

Field	Variable	Description	Units
1	Line	Line Number	
2	Fiducial	Seconds after Midnight	sec.
3	X_NAD83	Easting (X) in NAD83 Alberta 10TM Projection	m
4	Y_NAD83	Northing (Y) in NAD83 Alberta 10TM Projection	m
5	GPS_Z	GPS Elevation (above WGS84 datum)	m
6	Radar	Radar Altimeter	m
7	DTM	Terrain (above WGS84 datum)	m
8	Hz_monitor	Powerline Monitor (60 Hz)	μV
9 – 159	Resistivity	Resistivity at Depth Below Surface from 0 – 300 m at 2 m intervals	ohm-m
	Depth*	Depth Below Surface (0 – 300 m)	m
	Distance*	Distance Along Line	m

Note – The Depth and Distance fields are in the Geosoft database only.

The null values in the ASCII archive are displayed as \*.

**Grid Archive File Description:**

The grids are in Geosoft format. A grid cell size of 200m was used for all area grids.

File	Description	Units
ERDA_Northeast_RMI.grd	Residual Magnetic Intensity	nT
ERDA_Northeast_VD1.grd	First Vertical Derivative	nT/m
ERDA_Northeast_Res_z.grd	Apparent Resistivity from dB/dt Z	ohm-m
ERDA_Northeast_RDI_Slice_(0 to 120)m(_deh).grd	Resistivity Depth Slices for 0 to 120 m depths	ohm-m
ERDA_COMBINED_RMI.grd	Residual Magnetic Intensity merged with previous surveys	nT
ERDA_COMBINED_VD1.grd	First Vertical Derivative merged with previous surveys	nT/m
ERDA_COMBINED_30Hz_Res_z.grd	Apparent Resistivity from dB/dt Z merged with previous surveys	ohm-m
ERDA_90Hz_Res_z.grd	Apparent Resistivity from dB/dt Z for the 90Hz area only	ohm-m
ERDA_COMBINED_RDI_Slice_(0 to 120)m(_deh).grd	Resistivity Depth Slices for 0 to 120m depths merged with previous surveys	ohm-m

The \*\_deh files are the grid files corrected for asymmetry (“de-herringboned”).

---

### Resistivity Depth Section grid archive Description:

The resistivity depth section grids are named according to the following convention:

*rdi***LINE***\_raw(or\_trc).grd*

where **LINE** is the line number of the section grid and **trc** refers to sections that are terrain corrected. Grids are in Geosoft binary format with units in ohm-metres.

### SEG-Y Archive Description:

Two sets of the resistivity SEG-Y files were archived. One set relative to surface and one set shifted to be referenced to a datum of 885 metres, above the WGS84 spheroid. Both the shifted and non-shifted SEG-Y files have identical names and are differentiated by the directories in which they are contained (surface, datum). The SEG-Y files are named according to the following convention:

*sgy***LINE***.sgy*

where **LINE** is the survey line number.

# Appendix B

---

## Map Product Grids

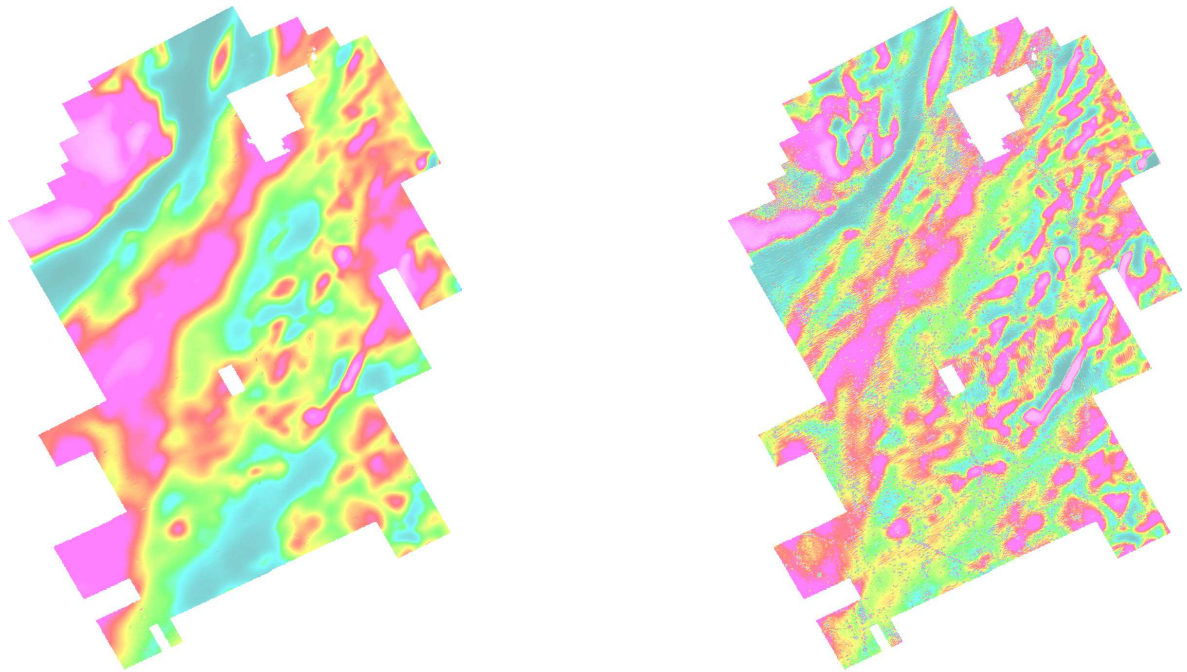


Figure 1. Residual Magnetic Intensity (left) and First Vertical Derivative of Residual Magnetic Intensity (right)

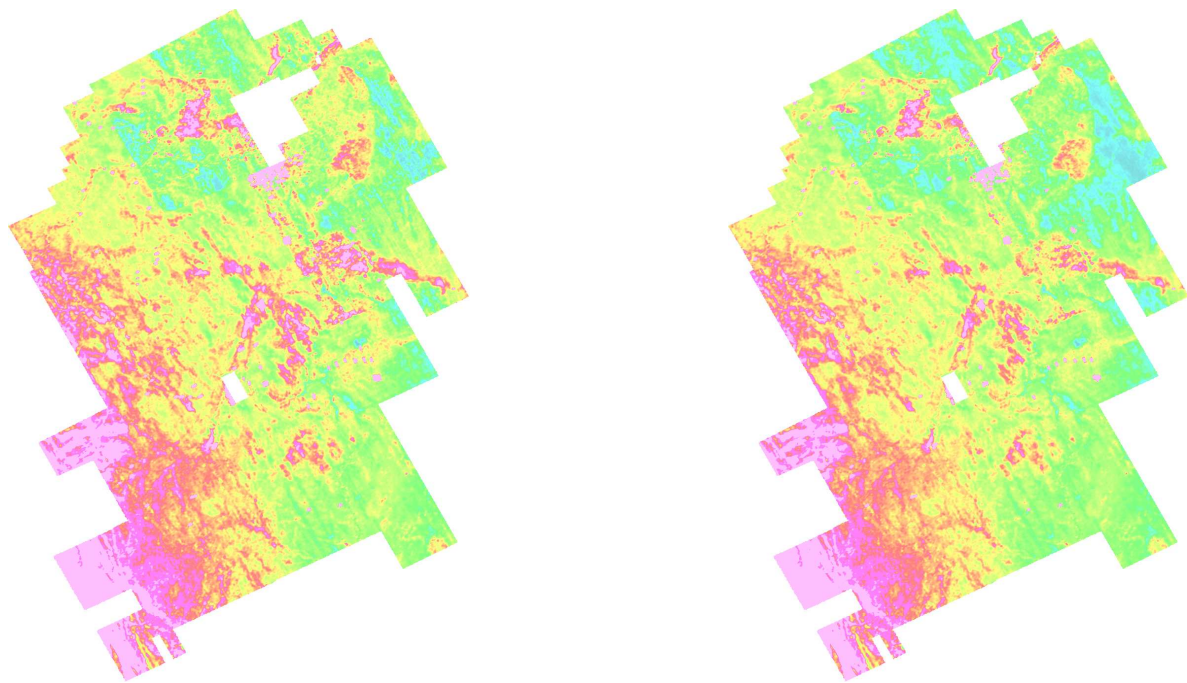


Figure 2. Resistivity Depth Slices at 0 metres (left) and 10 metres (right)

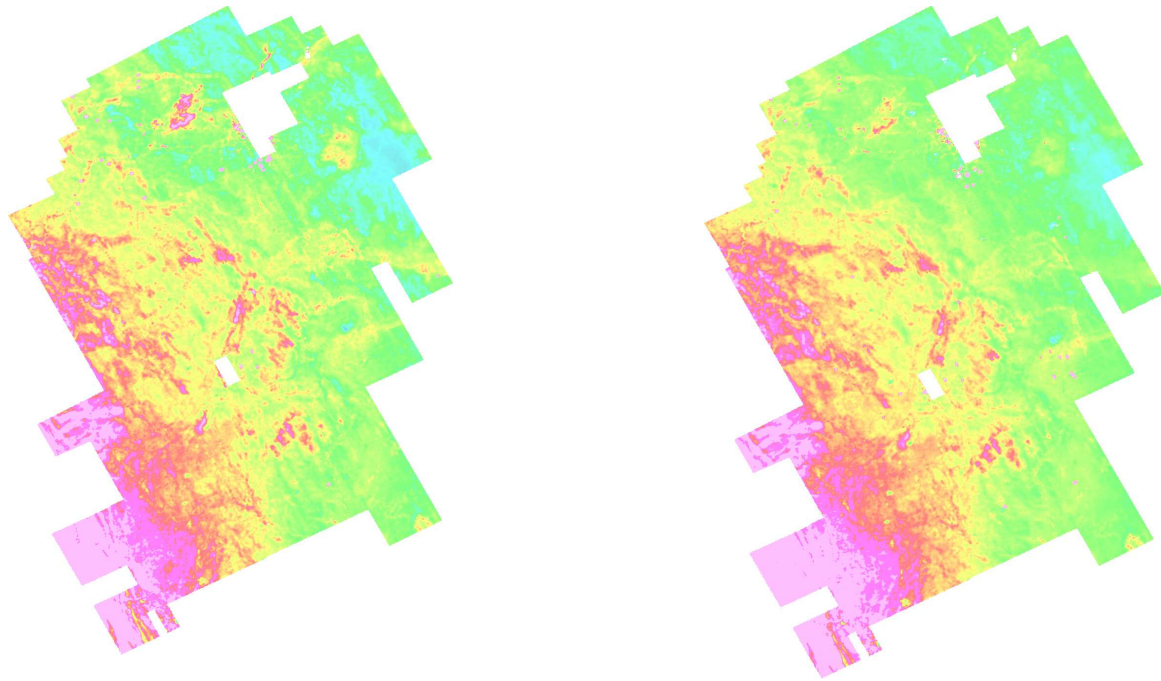


Figure 3. Resistivity Depth Slices at 30 metres (left) and 60 metres (right)

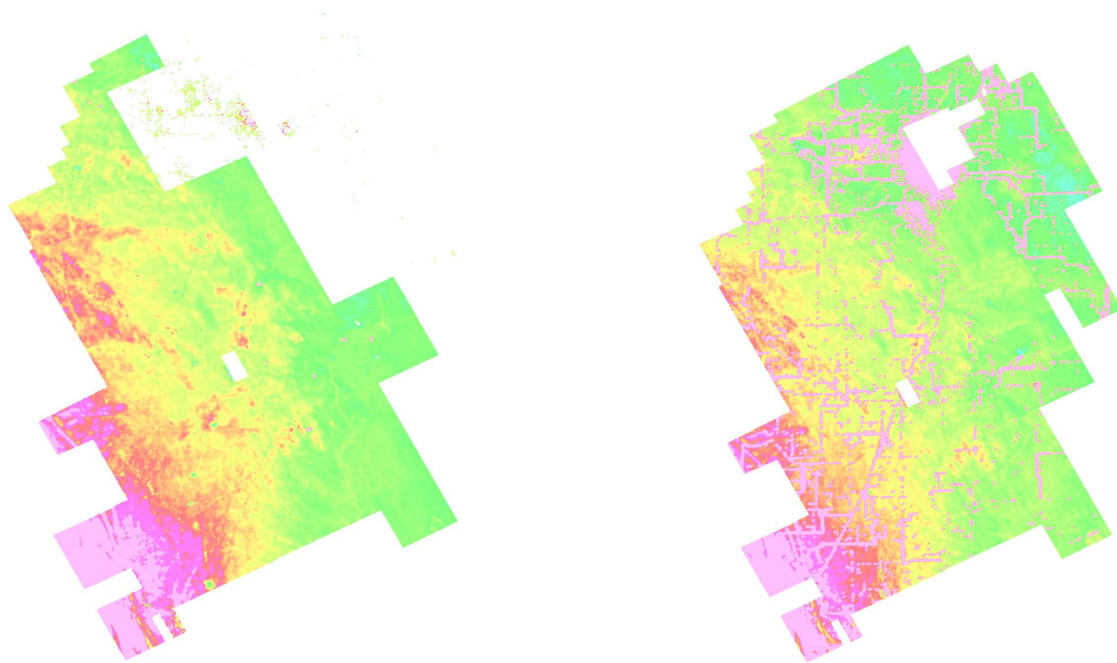


Figure 4. Resistivity Depth Slices at 120 metres (left) and Apparent Resistivity Derived from dB/dt Z Coil Channels 1 to 30 (right)

---

## Appendix C

### Reference Waveform

## Reference Waveform Descriptor:

The information shown is only an example. The actual reference waveforms are provided on CD-ROM or DVD and will have been renamed to ptaFLTpre.out / ptaFLTpost.out, "FLT" represents the flight number.

The reference waveform can be divided into four main sections, which are described below.

### Section 1

This section contains the name of the raw reference waveform file (i.e. **D0051612.002**). The approximate horizontal and vertical offsets (i.e. **125 m** and **50 m**) of the EM bird position in meters are listed. These are followed by the base frequency (i.e. **30 Hz**) in Hertz and the sample interval (i.e. **8.14 μs**) in microseconds.

```

GEOTEM Calibration Data - Version 31 July 1998
'D0051612.002' = Name of original saved parameter table file
125.0000000 = Horizontal TX-RX separation in meters
50.0000000 = Vertical TX-RX separation in meters
30.0000000 = Base Frequency in Hertz
8.1380208 = Sample Interval in micro-seconds
  
```

### Section 2

This section displays the gate configuration for channels 1 to 30.

30 Time Gates: First and Last Sample number, RMS chart position:

Start & end samples of each channel

1	1029	1041	1
2	1042	1043	2
3	1044	1045	3
4	1046	1049	4
5	1050	1054	5
6	1055	1060	6
7	1061	1067	7
8	1068	1075	8
9	1076	1085	9
10	1086	1097	10
11	1098	1111	11
12	1112	1127	12
13	1128	1145	13
14	1146	1165	14
15	1166	1187	15
16	1188	1211	16
17	1212	1237	17
18	1238	1265	18
19	1266	1295	19
20	1296	1330	20
21	1331	1370	21
22	1371	1415	22
23	1416	1465	23
24	1466	1520	24
25	1521	1580	25
26	1581	1650	26
27	1651	1730	27
28	1731	1820	28
29	1821	1920	29
30	1921	2048	30

Channels 1 to 30

### Section 3

This section contains the different types of conversion factors for each of the components. If the data are provided in ppm the standard procedure is to normalize the data based on the individual components. Three different conversion factors are provided. The first factor converts the data to ppm based on the peak voltages of each individual component. The second factor converts the data to ppm based on the “total” peak voltage which is actually the RMS value of the 3 components. The third factor converts each component to standard SI units, which are teslas per second for the dB/dt data and teslas for the B-field data.

Component:						
	dBx/dt	dBy/dt	dBz/dt	Bx	By	Bz
IndivPPM_per_DataUnit:	0.1112428E-01	1.106797	0.2890714E-01	0.1519028E-01	1.670836	0.3945841E-01
TotalPPM_per_DataUnit:	0.1038160E-01	0.1038160E-01	0.1038160E-01	0.1417559E-01	0.1417559E-01	0.1417559E-01
SI_Units_per_DataUnit:	0.1000000E-11	0.1000000E-11	0.1000000E-11	0.1000000E-14	0.1000000E-14	0.1000000E-14

### Section 4

The last section contains the reference waveform. Each column represents a component (i.e. dBx/dt). The data units (i.e. pT/s) for each component are displayed in the second row. The first column is the sample number. The transmitter channel (TX) values have been converted to transmitter moment value (transmitter current x loop area x number of turns)

For this example there are 2048 samples.

Component:	TX	dBx/dt	dBy/dt	dBz/dt	Bx	By	Bz
DataUnits:	Am <sup>2</sup>	pT/s	pT/s	pT/s	fT	fT	fT
2048 Samples:							
1	-54.0157	2173.5072	-5247.0123	-644.5732	990.3759	1257.3142	-12103.1713
2	-57.8884	3468.3254	-2344.3560	306.4653	1018.6012	1238.2357	-12100.6771
3	-71.5363	5721.1583	1205.4813	4170.6932	1065.1601	1248.0460	-12066.7360
4	-206.1874	4060.4902	5604.6317	4724.2987	1098.2045	1293.6566	-11946.9083
	●	●	●	●	●	●	●
	⋮	⋮	⋮	⋮	⋮	⋮	⋮
	▼	▼	▼	▼	▼	▼	▼
2045	54.8685	-3090.8335	3564.9971	-133.8272	-2049.2539	-1334.6109	11487.9835
2046	51.0590	-3645.2052	2610.5802	973.5404	-2078.9186	-1313.3659	11495.9063
2047	49.5162	-2219.4477	3085.7474	1436.8767	-2096.9806	-1288.2541	11507.6001
2048	51.3619	-1019.7309	5148.7879	1226.6542	-2105.2792	-1246.3531	11517.5823